Journal of Science and Technology in Civil Engineering, HUCE, 2024, 18 (3): 125–143

NUMERICAL INVESTIGATION ON BEHAVIOUR OF MOORING LINE SYSTEM FOR CONTAINER SHIP AT BERTH

Vu Minh Tuan[a,*], Thai Duy Loi[b]

[a]*Faculty of Hydraulic engineering, Hanoi University of Civil Engineering, 55 Giai Phong road, Hai Ba Trung district, Hanoi, Vietnam*
[b]*Coastal & River Engineering Research Center, Portcoast Consultant Corporation, 92 Nam Ky Khoi Nghia road, District 1, Ho Chi Minh city, Vietnam*

Article history:
Received 02/4/2024, Revised 29/5/2024, Accepted 07/8/2024

Abstract

The constant growth of the world's maritime industry has led to the need to increase the size of ships as well as accelerate the trend of moving ports to open sea areas and outside estuaries. Increasing the size of ships, especially container ships, has the potential to cause unsafe ship anchoring in ports. Furthermore, the mooring of ships at the harbor also lacks international guidelines on the layout of the mooring system. Meanwhile, relocating seaports outside estuaries and open seas can create conditions for high winds, high tidal fluctuations and strong currents to penetrate the port basin. This paper presents a study using the MIKE 21 MA numerical model to determine the most optimal mooring layout for a container ship as well as clarify the influence of factors (wind, current, water level and ship's draft) on the tension force of the mooring lines. The most optimal mooring layout in the study scenarios was uncovered from the simulation results. In addition, wind was identified as the factor with the greatest influence on the tension force of the mooring system.

Keywords: container ship; wind; mooring force; angle of mooring line; mooring layout; numerical model.

https://doi.org/10.31814/stce.huce2024-18(3)-10

1. Introduction

Researching the motion of ships moored at the berth under the impacts of waves, wind, currents... is a very important issue for all port design and operation projects because the ship's dynamic behavior directly affects the safety of cargo loading and unloading operations as well as the integrity of auxiliary equipment (mooring lines, bollards and fenders). In addition, natural conditions (waves, wind, currents...) are the main factors that can affect the port's downtime as well as its efficiency [1]. Therefore, it is very necessary to specifically determine the limits of these conditions that affect the movements of ships moored in the berth within the safe threshold that allows the berth to operate in order to improve operational efficiency and minimize the risk of accidents. Besides, the movements of ships moored in the berth depend greatly on the mooring line system. Understanding the behavior of ship mooring lines in response to operating conditions will provide necessary information for the design [2], selection of mooring lines and more optimized operation of ship mooring lines.

Currently in the world, investigating and assessing the behavior of mooring line systems and ships at ports is mainly carried out through experimental studies as well as numerical models. The use of physical models to study the dynamic behavior of ships moored at berths is a classic approach described in detail in a number of standards and design guidance documents [3, 4]. The outstanding advantage of this method is that the physical processes occurring in the model are most similar to reality, and physical quantities (ship motions, mooring force, elongation of mooring line, etc.) could

*Corresponding author. *E-mail address:* tuanvm@huce.edu.vn (Tuan, V. M.)

be measured and observed intuitively with high precision [5, 6]. However, this method has the biggest disadvantages: high cost and time consuming to build and setup experimental models. Along with the development of computer technology and the achievements of theoretical research, many numerical models have been developed to perform dynamic mooring analysis of ships in ports. One of the first studies that used numerical simulation method to clarify the behavior of a 200,000 DWT oil tanker moored in a sea port exposed to waves was carried out by Oortmerssen [7]. Next, Molen [8] developed and tested numerical models to determine the behavior of ships moored in harbor under the impact of long-period and nonlinear waves. Van der Ven [9] applied a series of numerical models to determine the movements of an oil tanker moored in Berth A of the Leixoes port, Portugal under the influence of random waves. Terblanche et al. [10] applied the Surfbeat module of the Delft3D numerical model to simulate longwave penetration in the Ngqura harbor in South Africa and then the results of this longwave model were used as input into a ship motion simulation model to calculate low-frequency forces on a 9000 TEU container ship. Van der Molen et al. [11] proposed to optimization measures to reduce long wave energy, reduce mooring force and reduce ship movements moored at Berth 5 of the Geraldton port (Australia) by applying set of numerical models. Following this, Pierre-Demenet et al. [12] performed a simulation of an LNG tanker moored at a berth subjected to wave impacts using the DiodoreTM numerical model and then compared with the experimental results. Huang et al. [13] conducted a simulation of an oil tanker moored at the berth using Optimoor model with water level, wave, wind, and current conditions to determine 06 DOF ship motion components. Recently, Yan et al. [14] used a hybrid Boussinesq-panel model to simulate the hydrodynamic response of a moored container ship under harbor oscillations caused by irregular waves. These are very important studies for port operations as they contribute to improving the safety of moored ships and appropriate harbor design. However, these studies have some limitations such as often only considering the fixed mooring line layout, only pay attention to the movements of the moored ship without considering the mooring line response and the factors affecting the mooring force.

This article focuses on studying the behavior of the ship's mooring line system under the impacts of natural conditions (wind, current, and water level), the ship's draft and mooring layout by using the MIKE 21 MA numerical model. From there, the optimal mooring layout could be determined as well as uncover the influence of these factors on the mooring force.

2. Methodology

2.1. Numerical model theory

MIKE 21 MA is an numerical model for solving the equations of motion for a vessel/floating body exposed to dynamic environmental forcing in the time-domain. The basis for a MIKE 21 MA simulation, is always the output file generated which contains the bundled set of various data relevant for a vessel submerged to a certain draft (geometric and frequency response data etc.), all of which is necessary for MIKE 21 MA as input [15].

The motion equation of the floating body [15] could be solved in the time domain as followed:

$$\sum_{k=1}^{6}\left(M_{jk}+a_{jk}\right)\ddot{x}_k(t)+\int_0^t K_{jk}(t-\tau)\,\dot{x}_k(\tau)\,d\tau+C_{jk}x_k(t)=F_{jD}(t)+F_{jnl}(t) \tag{1}$$

where $x_k(t)$ is six rigid-body degrees of freedom; M_{jk} is the inertia restoring matrix; C_{jk} is the hydrostatic restoring matrix; a_{jk} is impulsive (added mass) contributions; K_{jk} is the radiation impulse response function; $F_{jnl}(t)$ non-linear external forces from the mooring system and viscous and frictional damping (Froude-Krylov force); $F_{jD}(t)$ is the wave exciting forces.

Wind forces are calculated according to the following formula [15]:

$$\begin{aligned} F_{x,w}(t) &= \frac{1}{2} C_{x,w} \rho_{\text{air}} V_w(t)^2 A_{T,w} \\ F_{y,w}(t) &= \frac{1}{2} C_{y,w} \rho_{air} V_w(t)^2 A_{L,w} \\ M_{xy,w}(t) &= \frac{1}{2} C_{xy,w} \rho_{air} V_w(t)^2 A_{L,w} L_{PP} \end{aligned} \tag{2}$$

where $F_{x,w}(t)$ is the force due to wind in x direction, over time t; $F_{y,w}(t)$ is the force due to wind in y direction, over time t; $M_{xy,w}(t)$ is the moment due to wind, over time t; $C_{x,w}$, $C_{y,w}$, $C_{xy,w}$ are the wind drag coefficients; ρ_{air} is the density of air; $V_w(t)$ is the wind speed over time t; $A_{T,w}$ is the transversal windage area; $A_{L,w}$ is the longitudinal windage area; L_{PP} is the length between perpendiculars.

Current forces are derived based on [15] as follows:

$$\begin{aligned} F_{x,c}(t) &= \frac{1}{2} C_{x,c} \rho_{\text{water}} V_c(t)^2 L_{PP} T \\ F_{y,c}(t) &= \frac{1}{2} C_{y,c} \rho_{\text{water}} V_c(t)^2 L_{PP} T \\ M_{xy,c}(t) &= \frac{1}{2} C_{xy,c} \rho_{\text{water}} V_c(t)^2 L_{PP} T \end{aligned} \tag{3}$$

where $F_{x,c}(t)$ is the force due to current in the x direction, over time t; $F_{y,c}(t)$ is the force due to current in the y direction, over time t; $M_{xy,c}(t)$ is the moment due to the current, over time t; $C_{x,c}$, $C_{y,c}$, $C_{xy,c}$ are the current drag coefficients; ρ_{water} is the density of water; $V_c(t)$ is the current speed over time t; T is the ship's draft.

2.2. *Numerical model calibration*

The calibration procedure aims to evaluate the reliability of the numerical model as well as the influence of the calibration parameters before running the main study scenarios. Normally, this work only compares with actual measured data. Due to limitations in real measurement data on dynamic ship mooring systems, this study will be compared and tested with the research results of Sáenz et al. [16]. They investigated the behavior of the mooring system of the Emma Maersk ship with a displacement of 183,000 tons in port. This ship was moored by a system of 16 mooring lines (12

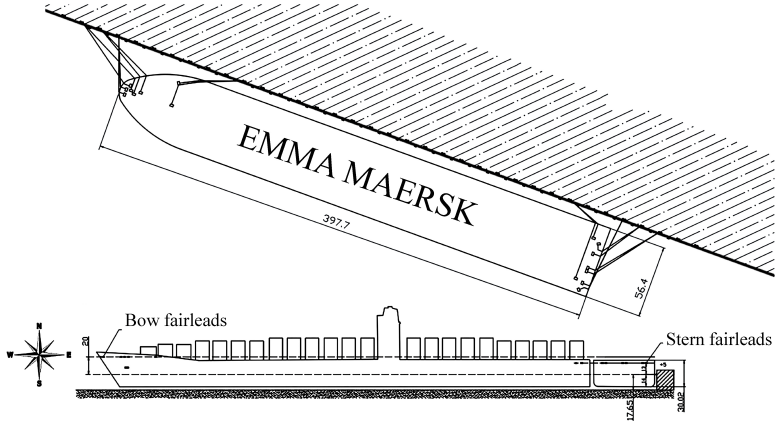

Figure 1. Ship mooring layout suggested by Sáenz et al. [16]

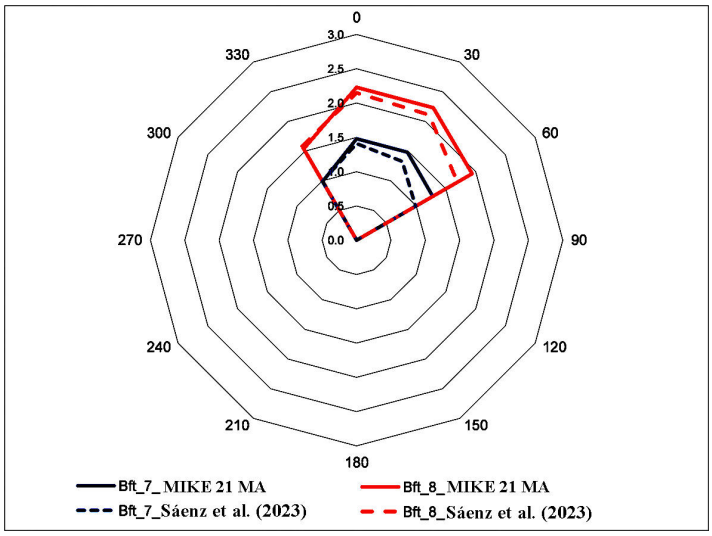

Figure 2. Comparison of significant sway motion results obtained by Sáenz et al. [16] and MIKE 21 MA model.

breast lines and 4 spring lines) according to International Association of Classification Societies (IACS) guidelines (Fig. 1). The results of this study could be compared with simulation results using MIKE 21 MA model (Fig. 2). Parameters of mooring line material and pre-tension force are used to calibrate the numerical model.

The comparison results in Table 1 show that the difference between the simulation and the values obtained by Sá Meanwhile, in the case of level wind 8 (BFT 8), the statistical error is only less than 14.5%. This small difference may be due to differences in mooring line conditions between the two works. However, for numerical simulation, this difference is acceptable. The pre-tension value of 5 tons obtained after calibration will be used to run the main scenarios.

Table 1. The difference between significant sway motion results simulated by the MIKE 21 MA model and the work of Sáenz et al. [16]

Wind direction (°N)	0	30	60	90	120	150	180	210	240	270	300	330
BFT 7	0.071 (5.1%)	0.154 (11.6%)	0.288 (29.0%)	-	-	-	-	-	-	-	-	-0.002 (-0.2%)
BFT 8	0.082 (3.8%)	0.120 (5.7%)	0.245 (14.5%)	-	-	-	-	-	-	-	-	-0.045 (-2.8%)

2.3. Study scenarios

This study uses a simulated ship, Emma Maersk, with a displacement of 183,000 tons. Details of the simulated ship parameters are shown in Table 2.

Table 2. The main dimensions of the Emma Maersk simulated ship

Ship	Deadweight (DWT)	Displacement (ton)	L_{OA} (m)	L_{PP} (m)	B (m)	h (m)	T (m)
Emma Maersk	174,239	183,000	397.7	376	56.6	37.2	14

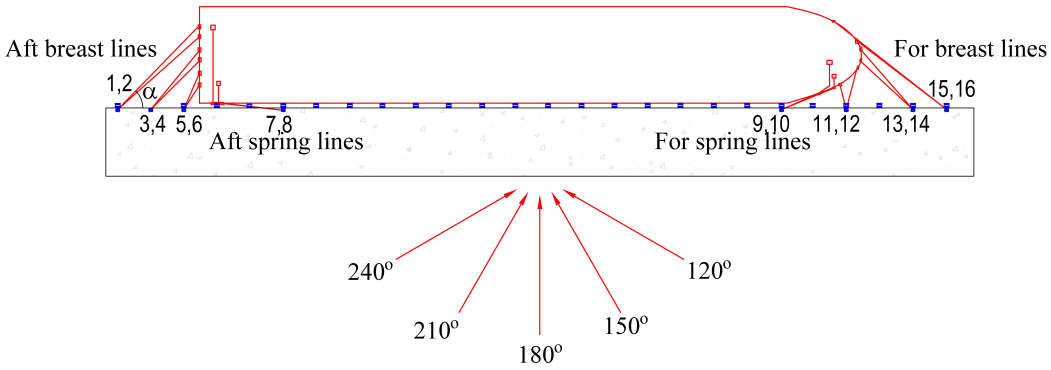

Figure 3. The general mooring layout of ship at berth

The most basic and most common mooring layout [17] with angle of No. 1 and 2 mooring lines of $\alpha = 46.7°$ for a simulated ship is depicted in Fig. 3 (MB1). From this layout, five other mooring layouts (MB2-MB6) are proposed based on the change of angle of mooring lines No. 1 and 2 (α = 36.7°, 40°, 50°, 55°, and 60°). All mooring lines are made from High Modulus Polyethylene (HMPE) material with line diameter of 42 mm and minimum breaking load of 1000 kN. In addition, all ship fenders used in the simulation were SPC 1400H cone fenders.

Regarding wind conditions, according to maritime regulations, when the wind is blowing at level 8 (BFT 8 > 20.7 m/s) or higher, all ships must leave the port and find a safe shelter. Therefore, the maximum wind speed value V_w = 20.7 m/s acts on the ship moored at the selected port. In order to determine the optimal layout of the ship's mooring system and determine the correlation between the angle of mooring line and the mooring force, all 6 layouts will be used to simulate with the same wind speed V_w = 20.7 m/s with effective wind directions varying from 120°N-240°N (30° interval) (Fig. 3). In addition, these simulations will also use the same high water level and full load draft T = 14 m.

For analyzing the influence of factors on mooring force, the basic mooring layout (MB1) is chosen to simulate with the combination of natural conditions in Cai Mep port area, Ba Ria-Vung Tau province, Vietnam, as follows: Wind - simulate 03 wind levels ($0.6V_w$; $0.8V_w$; $1.0V_w$) in the same wind direction of 180°N; Current - simulate 03 current speed levels ($0.6V_c$, $0.8V_c$ and $1.0V_c$ with V_c = 1.5 m/s); Water level - simulate 03 water level cases (High water level-HWL = +4.0 mCD (Chart Datum), Mean water level-MWL = +2.0 mCD, and Low water level-LWL = 0 mCD); Ship's draft - simulate 03 draft cases ($0.6T$; $0.8T$; $1.0T$).

Based on the mooring line layouts and simulation conditions, main study scenarios are proposed and summarized in Tables 3 and 4.

Table 3. Summary of main study scenarios to analyze mooring line behavior and establish correlation between angle of mooring line and mooring force

No.	Case	Layout	WL	Wind	Current	Draft
1	KB01	MB1	HWL		-	14 m
2	KB02	MB2	HWL		-	14 m
3	KB03	MB3	HWL	20.7 m/s;	-	14 m
4	KB04	MB4	HWL	120°N-240°N (Δ = 30°)	-	14 m
5	KB05	MB5	HWL		-	14 m
6	KB06	MB6	HWL		-	14 m

Table 4. Summary of main study scenarios to analyze factors affecting the mooring line system

No.	Case	Layout	WL	Wind	Current	Draft
1	KB07	MB1	LWL	20.7 m/s; 180°N	-	14 m
2	KB08	MB1	MWL	20.7 m/s; 180°N	-	14 m
3	KB09	MB1	MWL	20.7 m/s; 180°N	-	80%×14 m
4	KB10	MB1	MWL	20.7 m/s; 180°N	-	60%×14 m
5	KB11	MB1	MWL	80%×20.7 m/s; 180°N	-	14 m
6	KB12	MB1	MWL	60%×20.7 m/s; 180°N	-	14 m
7	KB13	MB1	HWL	-	1.5 m/s - 270°N	14 m
8	KB14	MB1	MWL	-		14 m
9	KB15	MB1	LWL	-		14 m
10	KB16	MB1	HWL	-		80%×14 m
11	KB17	MB1	HWL	-		60%×14 m
12	KB18	MB1	HWL	-	80%×1.5 m/s - 270°N	14 m
13	KB19	MB1	HWL	-	60%×1.5 m/s - 270°N	14 m
14	KB21	MB1	HWL	20.7 m/s; 180°N	1.5 m/s - 270°N	14 m
15	KB22	MB1	HWL	80%×20.7 m/s; 180°N		14 m
16	KB23	MB1	HWL	60%×20.7 m/s; 180°N		14 m

3. Results and Discussion

3.1. Determinating the optimal mooring layout

The simulation results of different mooring layouts are presented from Figs. 4 to Fig. 9. Fig. 4 specifically shows the results of mooring force distribution for MB1 layout. It is easy to see that mooring line No. 12 (forward breast line) provides the highest mooring force in the case of wind direction of 150°N (angle with the ship's bow direction axis is 60°). This result is consistent with reality because the wind resistance coefficient in this wind direction is the largest and mooring line No. 12 has a large mooring angle and short mooring line. Meanwhile, mooring line No. 7 (aft spring) provides the smallest mooring force in the case of a wind direction of 150°N (angle with the ship's bow direction axis is 60°). It is that mooring line No. 7 is a aft spring, not directly affected by the wind, has a small mooring angle and a long mooring line.

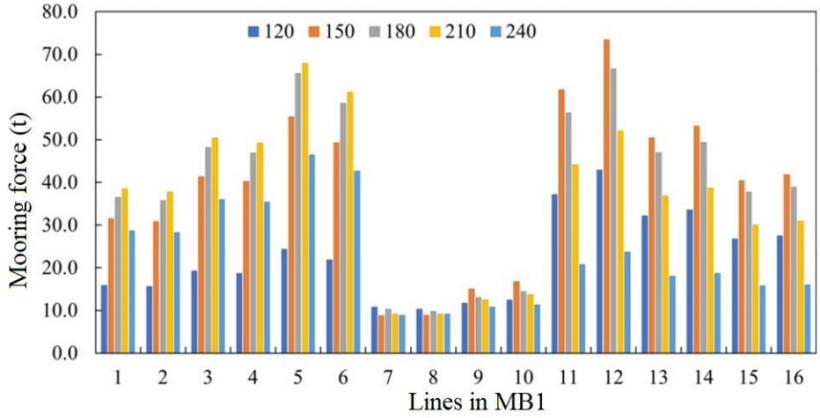

Figure 4. Comparison of mooring force between different wind directions - MB1 layout

The distribution of the mooring lines tension for MB2 layout is presented specifically in Fig. 5. The results show that mooring line No. 5 (aft breast line) gives the highest mooring force in the case of wind direction of 210°N (combined angle with steering axis 60°). This result is because the wind resistance coefficient in this wind direction is the largest and mooring line No. 5 has a large mooring angle and short mooring line. On the contrary, mooring line No. 9 (forward spring) gives the smallest mooring force in the case of wind direction of 240°N (angle to the ship's steering axis is 30°). The main reason for this phenomenon is that mooring line No. 9 is a forward spring, not directly affected by the wind, has a small mooring angle and a long mooring line.

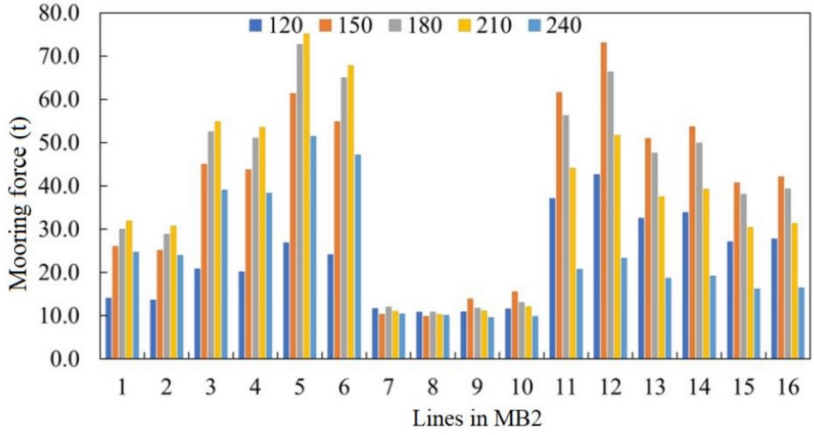

Figure 5. Comparison of mooring force between different wind directions - MB2 layout

Fig. 6 specifically describes distribution of the mooring lines tension for the MB3 layout. It shows that mooring line number 12 (forward breast line) provides the maximum mooring force in the case of a wind direction of 150°N (angle to the ship's bow direction axis is 60°). This result is consistent with reality because the wind resistance coefficient in this wind direction is the largest, mooring line No. 12 has a large mooring angle and short mooring line. Meanwhile, mooring line No. 8 (aft spring) provides the smallest mooring force in the case of a wind direction of 150°N (angle with the ship's bow direction axis is 60°). It is that mooring line No. 8 is a aft spring, not directly affected by the wind, has a small mooring angle and a long mooring line.

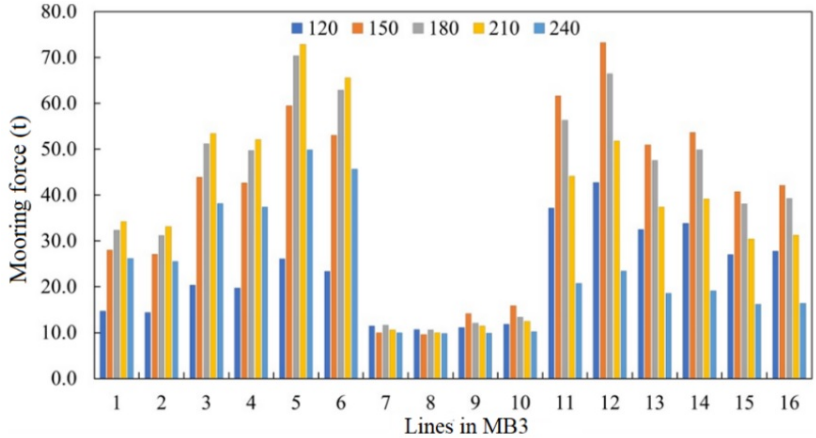

Figure 6. Comparison of mooring force between different wind directions - MB3 layout

The distribution of the mooring lines tension for MB04 layout is shown in Fig. 7. This figure shows that mooring line No. 12 gives the maximum mooring force in the case of wind direction of 150°N (angle with bow direction axis 60°). The wind resistance coefficient is greatest in this direction, along with the large mooring angle and short mooring line, causing high mooring line tension. In contrast, mooring line No. 7 provides the smallest mooring force in the case of wind direction of 240°N (angle to the ship's steering axis is 30°). This result comes from the fact that this is a spring line at the stern, not directly affected by the wind, has a small mooring angle and a long mooring line.

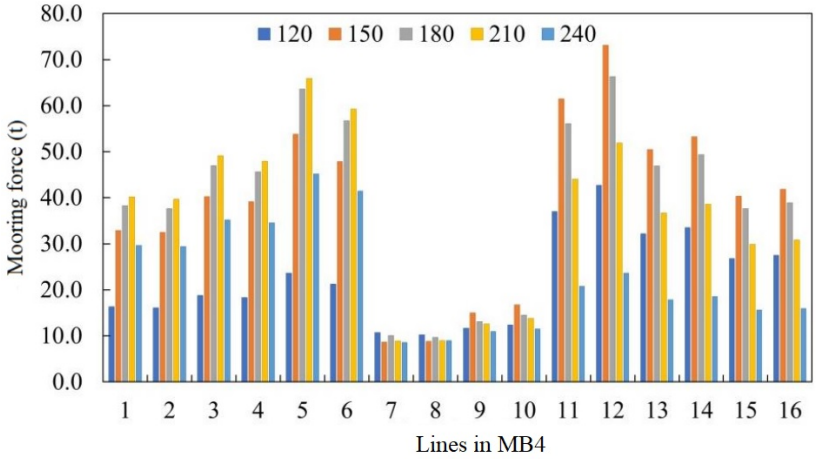

Figure 7. Comparison of mooring force between different wind directions - MB4 layout

Fig. 8 presents the results of the force distribution of the mooring lines for the MB5 layout. Once again, the largest mooring line tension corresponding to the case of 150°N wind direction (60° angle with the ship's bow direction axis) appears at mooring line No. 12. With this wind direction, the wind resistance coefficient is the largest and mooring line No. 12 has a large mooring angle and short mooring line. Meanwhile, mooring line No. 7 provides the smallest mooring line tension in the case of wind direction of 240°N (angle with the ship's steering axis is 30°). Because this is a aft spring with a small mooring angle and a long mooring line, it is not directly affected by the wind.

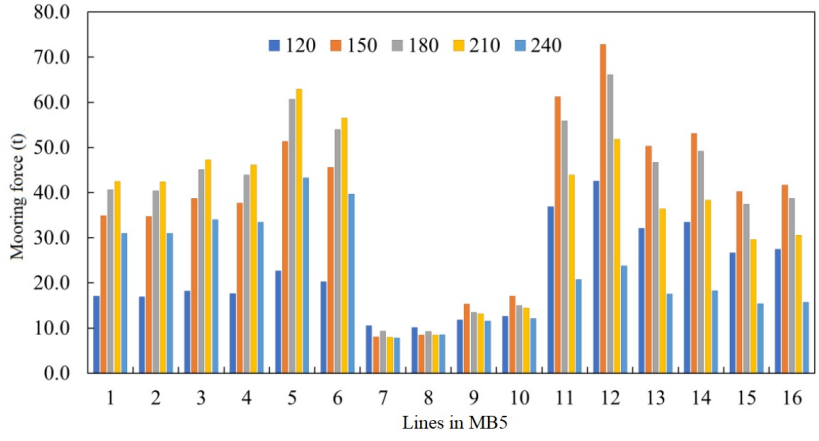

Figure 8. Comparison of mooring force between different wind directions - MB5 layout

The results of the force distribution of the mooring lines for the MB6 layout are shown in Fig. 9. It is easy to see that mooring line No. 12 gives the largest mooring force in the case of wind direction of 150°N (angle with the ship's bow direction axis is 60°). In contrast, mooring line No. 7 provides the

smallest mooring force in the case of a wind direction of 120°N (angle with the ship's bow direction axis is 30°).

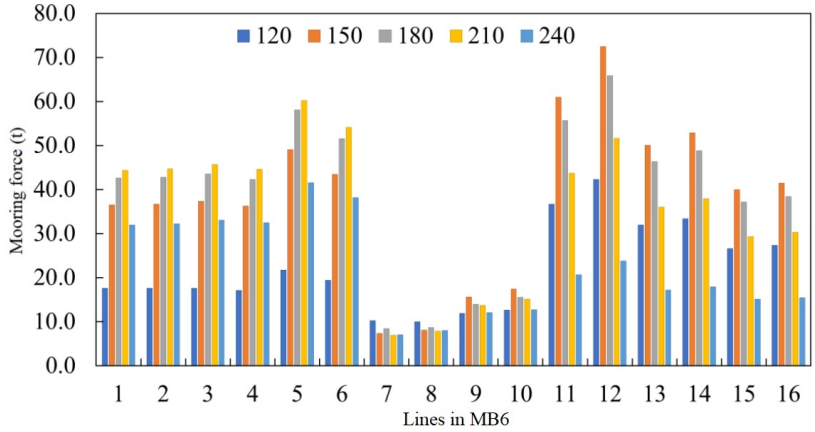

Figure 9. Comparison of mooring force between different wind directions - MB6 layout

When considering the tension force of the mooring lines for different layouts, the simulation results reveal that the maximum and minimum tension forces are relatively different in the same wind direction. Specifically, for the wind direction of 120°N (Fig. 10) the tension force difference of the mooring lines in each layout is not too much, especially for the spring lines and bow lines. The largest difference was recorded at mooring line No. 5 and 6 between MB2 and MB6, about 5.2 tons. It can be seen that this wind direction does not have much impact on mooring layout.

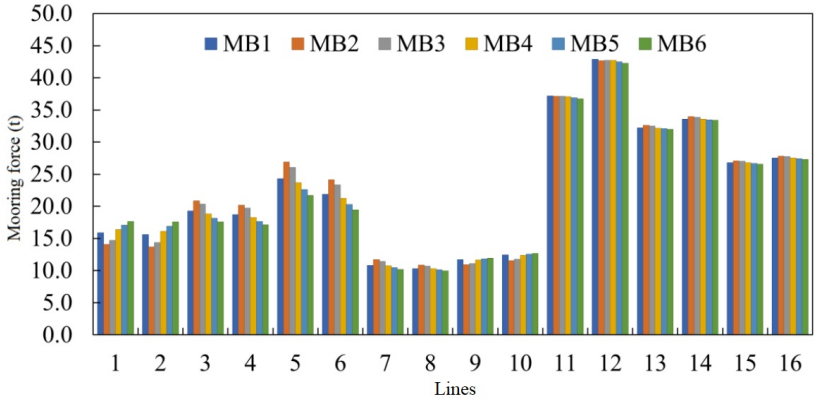

Figure 10. Comparison of mooring forces of 06 layouts - Wind direction of 120°N

Fig. 11 shows a comparison of the mooring line tension at different layouts in the same wind direction of 150°N. The results show that the tension force of the mooring lines on the bow and the spring lines of each layout does not change much, but the tension force of the mooring lines on the stern is different. The largest difference of about 6.32 tons is observed in mooring line No. 5 between MB2 and MB6. In addition, the tension force of the mooring lines in MB6 layout are quite difference and smaller than that of the other layouts.

Similar to the wind direction of 150°N, for the wind direction of 180°N (Fig. 12), the tension force of the mooring lines at the bow and the spring lines of each layout almost changes a lot, while the tension of the mooring lines at the stern is clearly. Specifically, the largest difference of approximately 14.63 tons occurs between MB2 and MB6 layout at mooring line No. 5. It is easy to see that MB6

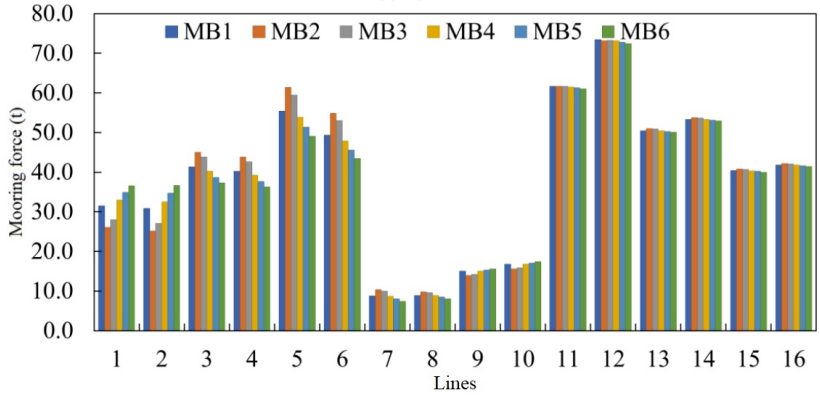

Figure 11. Comparison of mooring forces of 06 layouts - Wind direction of 150°N

layout distributes the tension of mooring lines in the mooring line group (bow, stern, spring) are relatively more uniform than the other layouts. In addition, this layout also usually provides smaller mooring force than the other layouts.

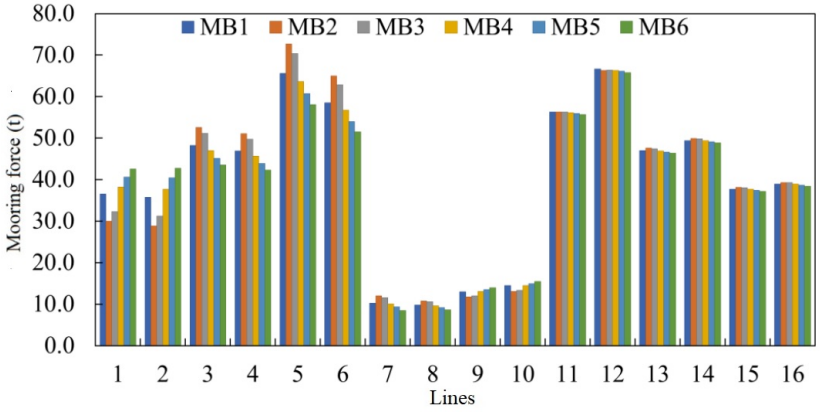

Figure 12. Comparison of mooring forces of 06 layouts - Wind direction of 180°N

When the wind direction is aligned with the ship's longitudinal axis at an angle of 60° (Fig. 13), the tension of the mooring lines at the bow and the spring lines of all layouts is almost unchanged.

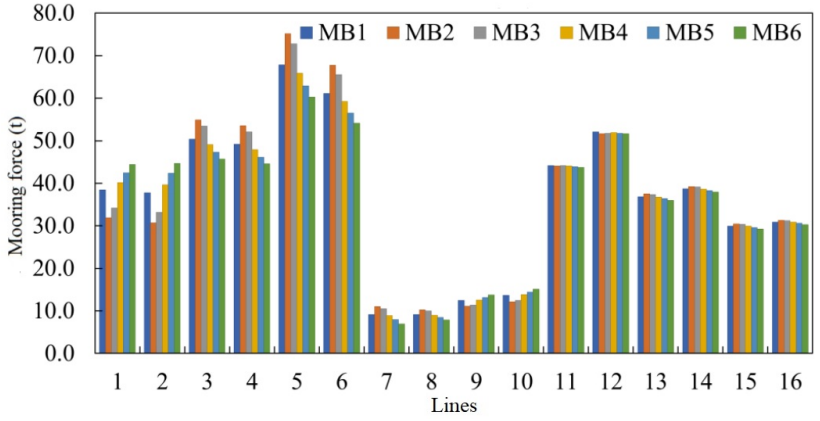

Figure 13. Comparison of mooring forces of 06 layouts - Wind direction of 210°N

However, the tension of the mooring lines on the stern is difference between the layouts. In general, the tension value of the stern line is larger than spring line group and bow line. Once again, the largest difference in mooring line tension appears at mooring line No. 5 between the MB2 and MB6 layout, which is about 15 tons. Besides, MB6 layout distributes the tension of the mooring lines relatively evenly and has smaller mooring line tension values than the other layouts. On the contrary, MB2 layout causes the greatest tension in the mooring lines in all layouts.

Trend of mooring line tension for wind direction of 240°N (Fig. 14) is similar to that for wind direction of 210°N. Specifically, the force of the mooring lines at forward spring and aft spring of the mooring layouts has a relatively small difference. Large difference is for the mooring lines on the stern. The tension force of mooring lines No. 5 between MB2 layout and MB6 layout is nearly 10 tons. Among the layouts, MB6 layout distributes the tension of mooring lines relatively evenly and the major of its value is smaller than the remaining layouts.

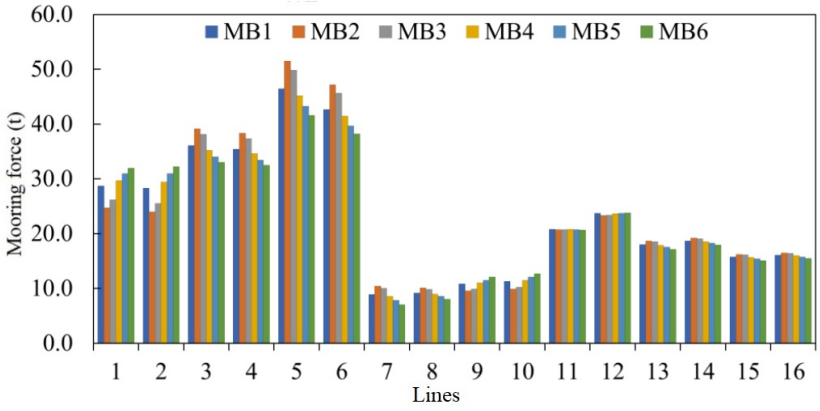

Figure 14. Comparison of mooring forces of 06 layouts - Wind direction of 240°N

In addition, the comparison between the mooring line groups in the bow and stern lines and forward spring and aft spring is also performed as in from Fig. 15 to Fig. 18. The results prove that the wind direction acts perpendicular to the ship (wind direction of 180°N), resulting in mooring forces being balanced and symmetrical. Meanwhile, the two main wind directions affecting the uneven mooring line system are the wind direction of 150°N and the wind direction of 210°N.

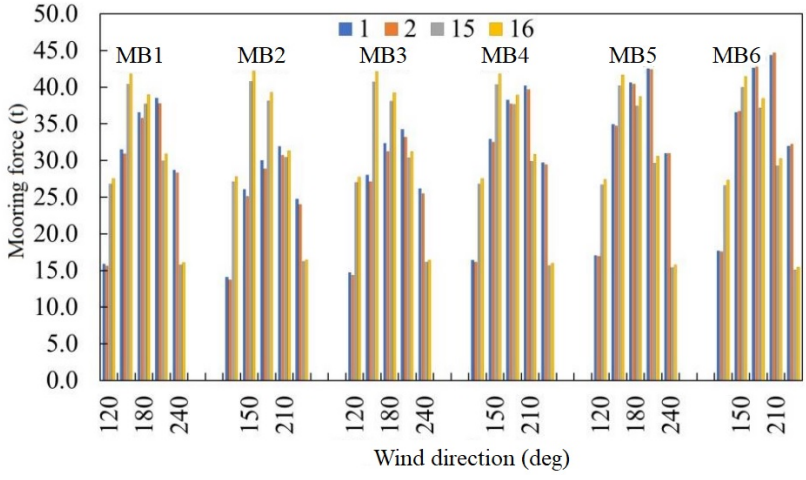

Figure 15. Comparison of No. 1, 2, 15, and 16 mooring forces - 06 layouts

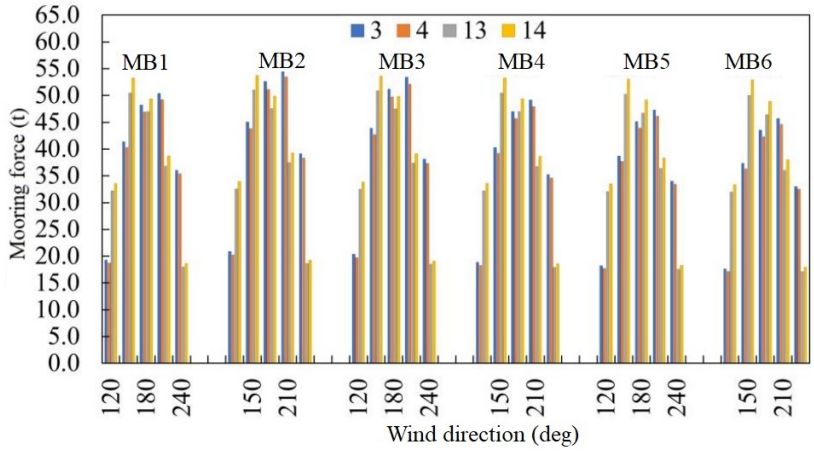

Figure 16. Comparison of No. 3, 4, 13, and 14 mooring forces - 06 layouts

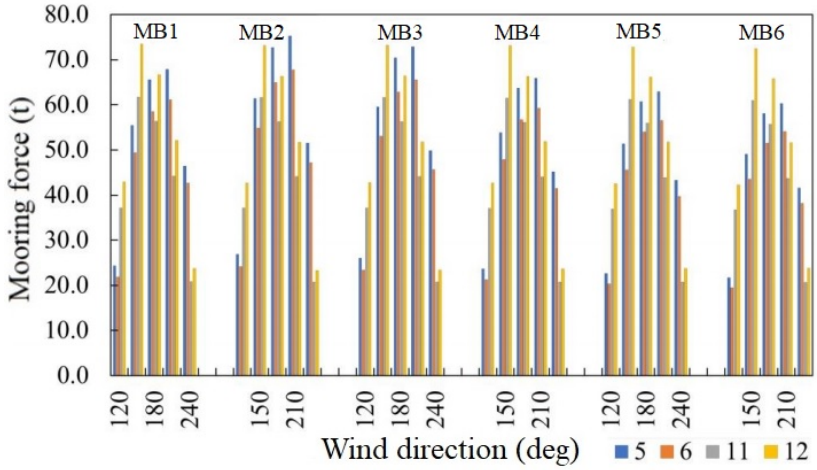

Figure 17. Comparison of No. 5, 6, 11, and 12 mooring forces - 06 layouts

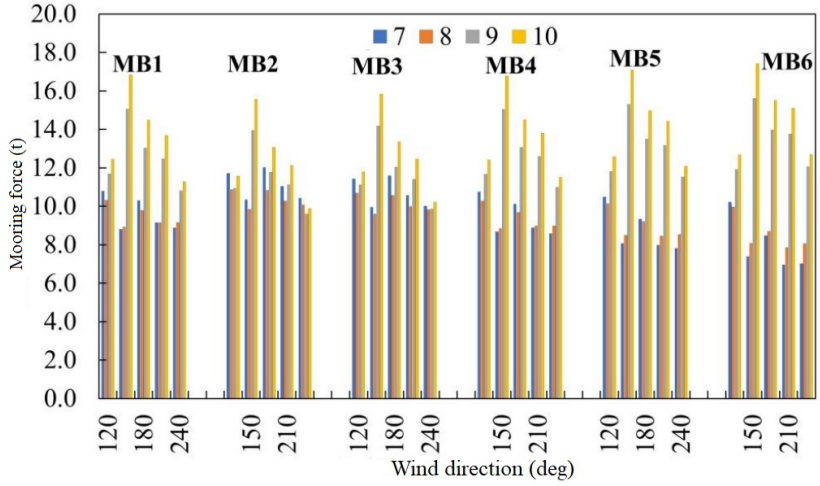

Figure 18. Comparison of No. 7, 8, 9, and 10 mooring forces - 06 layouts

3.2. Establishing the relationship between the angle of mooring line and the mooring force

Based on the simulation results, it is shown that the two main wind directions of 150°N (coordinated with the ship's longitudinal axis, 60° forward direction) and 210°N (coordinated with the ship's longitudinal axis, 60° steering direction) cause large and uneven distribution of mooring lines tension force. Due to its nearly symmetrical nature, the article only focuses on establishing the correlation between the angle of No. 1 and 2 mooring lines and the tension force of the mooring lines in the case of 210° wind direction. Details of the results are presented from Fig. 19 to Fig. 27 and Table 5. It is obvious that these correlations have very high coefficients of determination (R^2) in the range of 0.73-0.99. The R^2 coefficient of determination is a measure that provides information about the goodness of fit of a model. An R^2 of 1 means a perfect fit. These relationship equations can be used to serve

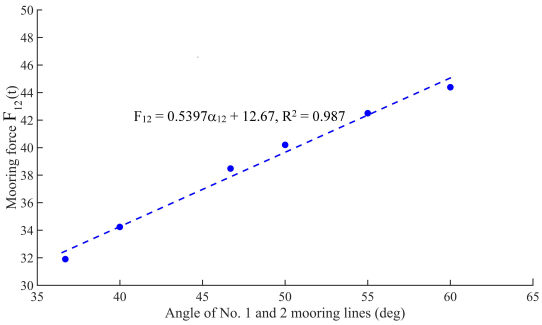

Figure 19. Relationship between angle of No. 1, 2 mooring lines and mooring forces of No. 1, 2 mooring lines

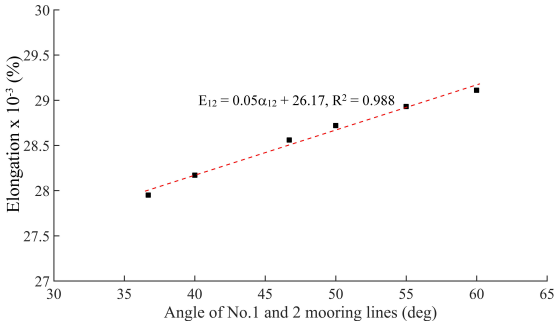

Figure 20. Relationship between angle of No. 1, 2 mooring lines and elongation of No. 1, 2 mooring lines

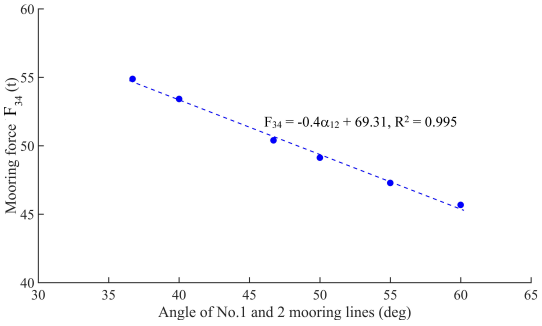

Figure 21. Relationship between angle of No. 1, 2 mooring lines and No. 3, 4 mooring forces

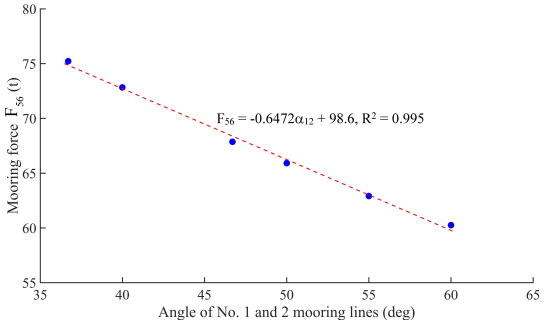

Figure 22. Relationship between angle of No. 1, 2 mooring lines and No. 5, 6 mooring forces

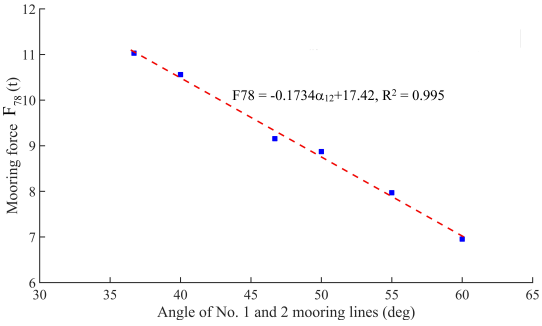

Figure 23. Relationship between angle of No. 1, 2 mooring lines and No. 7, 8 mooring forces

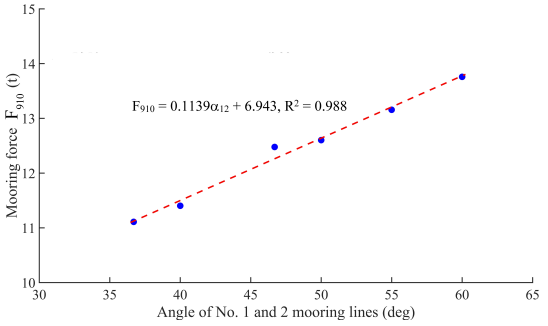

Figure 24. Relationship between angle of No. 1, 2 mooring lines and No. 9, 10 mooring forces

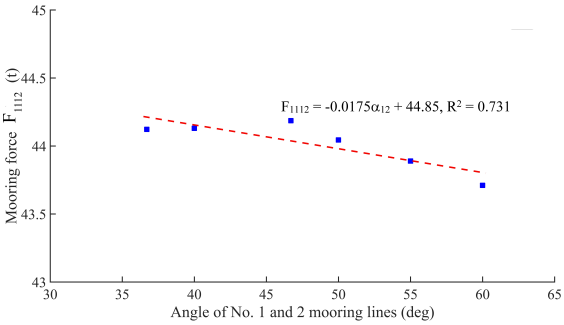

Figure 25. Relationship between angle of No. 1, 2 mooring lines and No. 11, 12 mooring forces

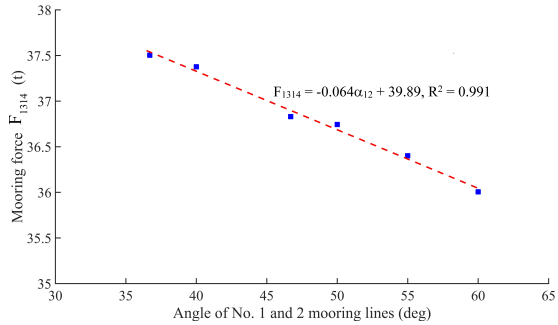

Figure 26. Relationship between angle of No. 1, 2 mooring lines and No. 13, 14 mooring forces

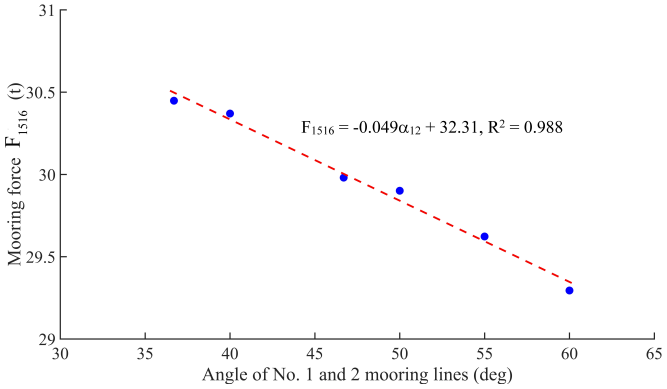

Figure 27. Relationship between angle of No. 1, 2 mooring lines and No. 15, 16 mooring forces

the design process of new ports as well as the operation of existing port facilities. Specifically, with a certain wind direction, the designer or operator can choose the appropriate values of angle of No. 1, 2 mooring lines to achieve the desired tension forces of the mooring lines from these correlation formulas.

Table 5. Summary of correlation between angle of mooring line of 1 and 2 and the mooring force in the mooring system

No.	Name of mooring line	The correlation formula between angle of mooring line with mooring force (elongation of mooring line)	R^2
1	Mooring line of 1, 2	$F_{12} = 0.5397\alpha_{12} + 12.67; E_{12} = 0.05\alpha_{12} + 26.17$	0.98
2	Mooring line of 3, 4	$F_{34} = -0.4\alpha_{12} + 69.31$	0.99
3	Mooring line of 5, 6	$F_{56} = -0.6472\alpha_{12} + 98.6$	0.99
4	Mooring line of 7, 8	$F_{78} = -0,1734\alpha_{12} + 17.42$	0.99
5	Mooring line of 9, 10	$F_{910} = 0.1139\alpha_{12} + 6.943$	0.98
6	Mooring line of 11, 12	$F_{1112} = -0.0175\alpha_{12} + 44.85$	0.73
7	Mooring line of 13, 14	$F_{1314} = -0.064\alpha_{12} + 39.89$	0.99
8	Mooring line of 15, 16	$F_{1516} = -0.049\alpha_{12} + 32.31$	0.98

3.3. Analyzing factors affecting mooring force

Based on main study scenarios, analysis results of changes in mooring force in basic layout of MB1 due to the impact of factors such as water level, ship's draft, current speed and wind speed is shown from Fig. 28 to Fig. 34. Fig. 28 shows the results of comparing the tension force of the mooring

lines in the case of constant wind, constant draft (14 m) and fluctuating water level. The results show that the tension force of most mooring lines varies proportionally to the water level. However, this rate of change is very small. Specifically, the largest increase in mooring force is only about 5 tons (11.5%) when the water level increases to 4.0 m (approximately 100%) at No. 3 and 14 mooring lines.

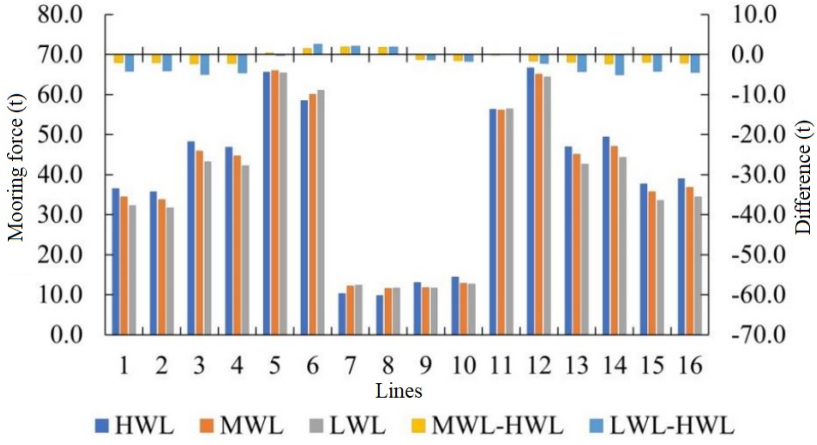

Figure 28. Comparison of mooring force affected by constant wind, constant water draft and variable water level (HWL, MWL, LWL) - MB1

Fig. 29 shows the change in tension force of the mooring lines when the ship's draft changes, fixed wind conditions (Wind direction of 180°N and wind speed of 20.7 m/s) and fixed water level (MWL). It is easily seen that the force of all mooring lines increases as the ship's draft increases. However, this increase is relatively small and the largest is only about 3.8 tons (approximately 6%) occurring at No. 5 mooring line when the draft increases by 40%.

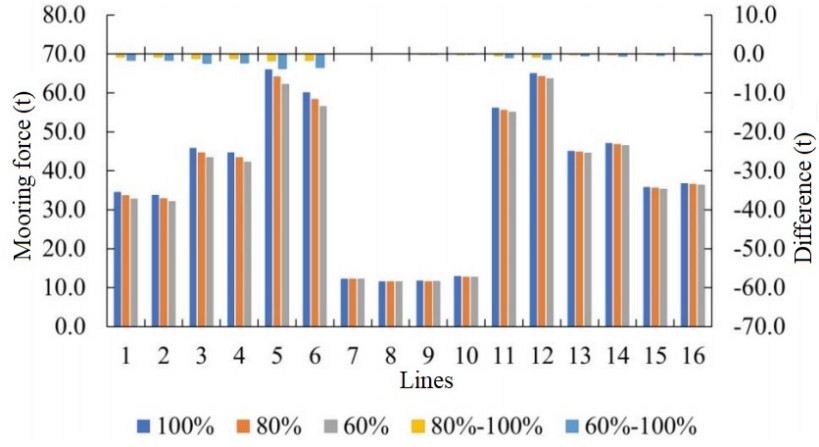

Figure 29. Comparison of mooring force in constant wind, constant water level and variable draft (100%, 80%, 60%) - MB01

Meanwhile, changing wind speeds will cause a very significant change in the tension force of each mooring line (Fig. 30). It is easy to observe that increased wind speed leads to increased mooring force. The largest increase in mooring force of about 45 tons (approximately 69%) occurs at No. 5 and No. 12 mooring lines when the wind speed increases by 40%. Therefore, wind speed greatly affects the tension force of the mooring lines.

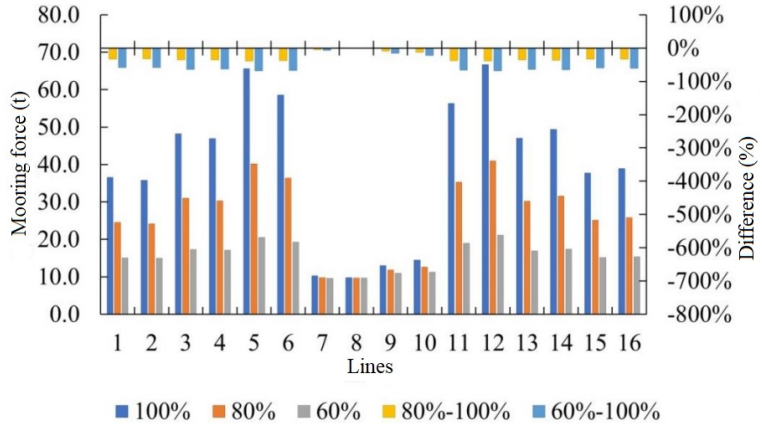

Figure 30. Comparison of mooring force in constant draft, constant water level and variable wind speed (100%, 80%, 60% with the same direction of 180°N) - MB1

Fig. 31 shows the impact of fixed current (with speed of 1.5 m/s and direction of 270°N), fixed draft (14 m) and only changing water level on the mooring force of MB1 layout. Simulation results demonstrate that in this case the tension force of each mooring line changes relatively small. The largest change recorded at No.7 mooring line between the LWL and HWL scenarios is 7 tons (about 31%). Therefore, when the mooring system is subjected to the combined impact of an unchanging current (speed and direction), the change in water level has a negligible on the force of most mooring lines.

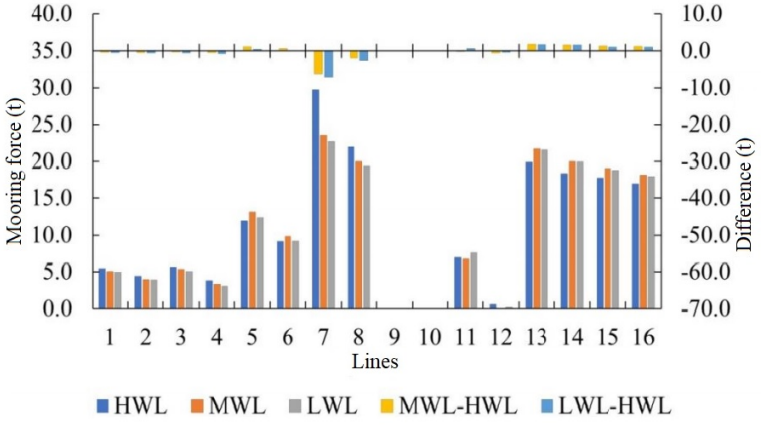

Figure 31. Comparison of mooring force in constant current, constant draft and variable water level (HWL, MWL, LWL) - MB1

The combined impact of variable draft, constant water level (HWL) and constant current (with speed of 1.5 m/s and direction of 270°N) on mooring force of MB1 layout is shown in Fig. 32. Simulation results reveal that in this case the tension force of each mooring line is almost unchanged.

In addition to the change in draft and water level, the variation of current on mooring force is also investigated and shown in Fig. 33. When the current speed decreases, the tension force of No. 7, 8, 13-16 mooring lines decreased accordingly and the tension force of the No. 7 mooring line decreased the largest by more than 14 tons (corresponding to nearly 90%) when the current speed decreased by 40%. Meanwhile, the stern lines (1-6) have increased tension force as the current speed decreases. The largest increase is about 4.4 tons (corresponding to 114%).

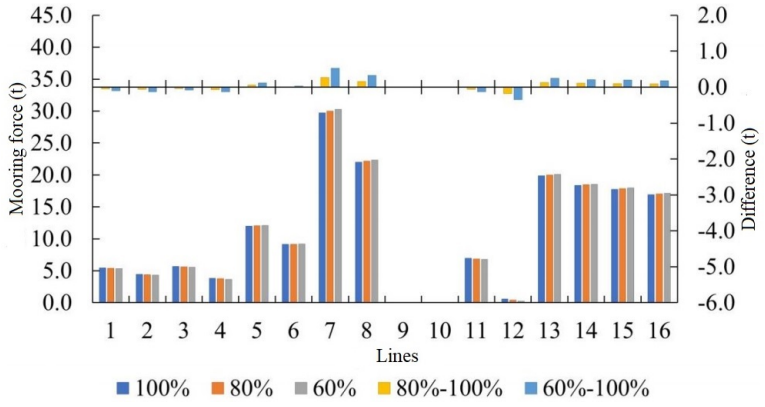

Figure 32. Comparison of mooring force in constant current, constant water level (HWL) and variable draft (100%, 80%, 60%) - MB1

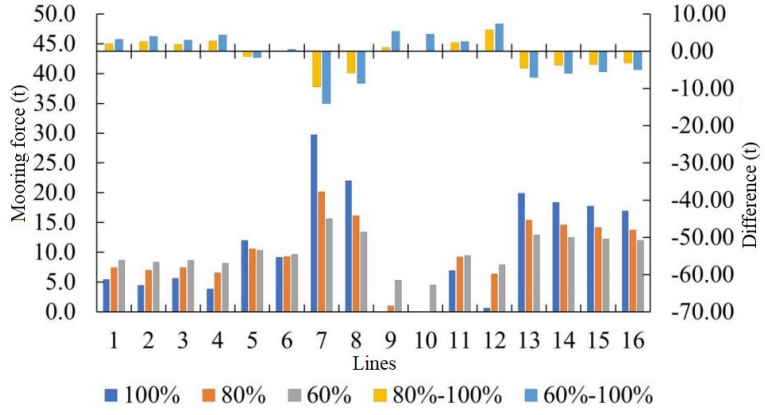

Figure 33. Comparison of mooring force in constant water level, constant draft and variable current speed: 100%, 80%, 60% (with constant current direction of 270°N) - MB01

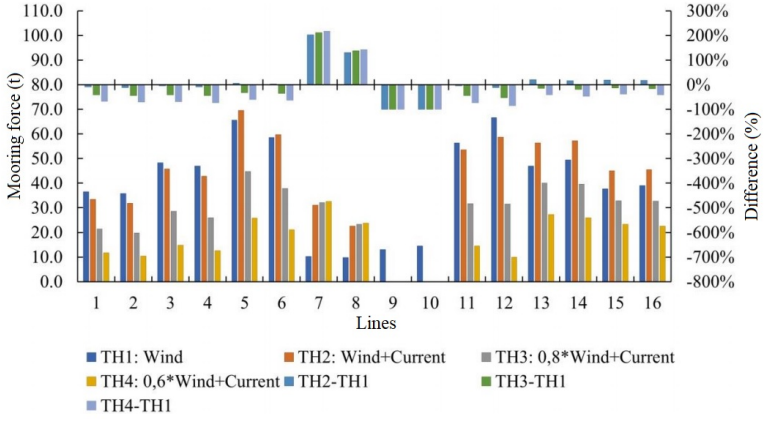

Figure 34. Comparison of mooring force due to wind and current conditions - MB1

However, when considering the impact of changing wind and constant current, the simulation results show that in this case, the tension force of most of mooring lines tends to decrease significantly as the wind speed decreases (Fig. 34). Therefore, when the mooring system is simultaneously affected by wind and current, the wind factor is still the main factor that significantly affects the tension force

of the mooring lines.

Based on the comments of each simulation case, the evaluation matrix of influencing factors is summarized and presented in Table 6. This table confirms that wind is the most influential factor on the mooring system, next to current factor and finally the water level and draft of the ship.

Table 6. Summary and assessment of factors affecting mooring force

Factor	Wind	Water level	Current	Draft
Wind				
Water level				
Current				
Draft				

Very Significant
Significant
Medium
Low
Quite low
Very low

4. Conclusions

In this study, the mooring force of a container ship moored at the port under the influence of factors (wind, current, water level and draft) is simulated by the MIKE 21 MA numerical model. A series of numerical simulations were conducted to investigate the influence of these factors on mooring force, thereby determining the optimal mooring line layout.

Some conclusions below can be drawn from the results of this study:

- Simulation results of 06 mooring layouts with 30 cases have shown that the MB6 layout with the angle of No. 1 and 2 mooring lines (stern line) of 60 degrees is the most optimal among the options with the mooring force being quite uniform between lines and having a small value than other options. This layout can be applied to existing berths by adding bollards or mooring winches to allow large tonnage ships to moor.

- The correlation equation between angle of No. 1 and 2 mooring lines (aft mooring lines) and the force of the mooring lines (or elongation) has been established and is highly reliable because it has a very good correlation coefficient R^2 = 0.73-0.99.

- Simulation results of 01 basic layout (MB1) for a moored ship with 12 cases confirmed that the wind factor is the main influencing factor on the mooring force in the mooring system and the second main factor is the current factor, other factors such as water level and ship's draft are secondary factors with insignificant influence. The two main wind directions that affect the mooring force are 150°N and 210°N.

The research results and proposed methods can be applied to the design and operation of ports receiving container ships moored in complex environments. However, this article only considers certain factors. Future research should consider material characteristics of mooring line, the wave impacts, and incorporating automatic mooring systems.

References

[1] Baker, S., Sultan, N., Cornett, A., Gunderson, W. (2017). Physical Modelling and Design Optimizations for a New Port in Brazil. In *Coastal Structures and Solutions to Coastal Disasters 2015*, American Society of Civil Engineers, 838–847.

[2] Baolei, G., Weiqian, L., Yan, L., Chongwei, Z. (2020). Study of the Influence with Different Berth Length for LNG Carrier Mooring. In *APAC 2019: Proceedings of the 10th International Conference on Asian and Pacific Coasts, 2019*, Hanoi, Vietnam, Springer, 101–106.

[3] Port and Airport Research Institute (2020). *Technical standards and commentaries for port and harbour facilities in Japan*.
[4] PIANC (2023). *Criteria for acceptable movement of ships at berths*. MarCom Working Group.
[5] Cornett, A. (2014). Physical modelling of moored ships for optimized design of ports and marine terminals. In *Proceeding of the 5th International Conference on Physical Modeling in Coastal and Port Engineering (Coastlab 2014)*, Varna, Bulgaria.
[6] Nguyen, X. P., Pham, N. D. K. (2019). Experimental Research on the Impact of Anchor-Cable Tensions in Mooring Ship at Vung Tau Anchorage Area. *International Journal on Advanced Science, Engineering and Information Technology*, 9(6):1892–1899.
[7] van Oortmerssen, G. (1977). The Behaviour of Moored Ships in Waves. In *Offshore Technology Conference*, 77OTC.
[8] van der Molen, W. (2006). *Behaviour of moored ships in harbours*. Delft University of Technology.
[9] Van der Ven, P. P. D. (2012). *The use of numerical models to determine the response of moored vessels to waves in a complex harbour geometry*. Delft University of Technology.
[10] Terblanche, L., van der Molen, W. (2013). Numerical modelling of long waves and moored ship motions. In *Coasts and Ports 2013: 21st Australasian Coastal and Ocean Engineering Conference and the 14th Australasian Port and Harbour Conference*, Engineers Australia Barton, ACT, 757–762.
[11] Van der Molen, W., Scott, D., Taylor, D., Elliott, T. (2015). Improvement of Mooring Configurations in Geraldton Harbour. *Journal of Marine Science and Engineering*, 4(1):3.
[12] Demenet, P.-F., Guisier, L., Marcol, C. (2018). Physical and numerical modelling of ship s moored in ports. In *34th PIANC World Congress*, Curran Associates, Inc. Panama, 214–227.
[13] Huang, J., Bing, X., Shao, R., Liu, Y., Li, X. (2019). Simulation research on mooring stability of oil tankers in Changxing Island Port Area considering open environmental conditions. *IOP Conference Series: Earth and Environmental Science*, 369(1):012006.
[14] Yan, M., Zheng, Z., Sun, Z., Ma, X., Dong, G. (2023). Numerical evaluation of the tension mooring effects on the hydrodynamic response of moored ships under harbor oscillations. *Ocean Engineering*, 288:116127.
[15] DHI (2024). *MIKE 21 Maritime-Frequency Response Calculator and Mooring Analysis*. Scientific Documentation.
[16] Sáenz, S. S., Diaz-Hernandez, G., Schweter, L., Nordbeck, P. (2023). Analysis of the Mooring Effects of Future Ultra-Large Container Vessels (ULCV) on Port Infrastructures. *Journal of Marine Science and Engineering*, 11(4):856.
[17] Van Zwijnsvoorde, T., Eloot, K., Vantorre, M., Lataire, E. (2019). A mooring arrangement optimisation study. In *11th International Workshop on Ship and Marine Hydrodynamics (IWSH2019)*, Hamburg, Germany.